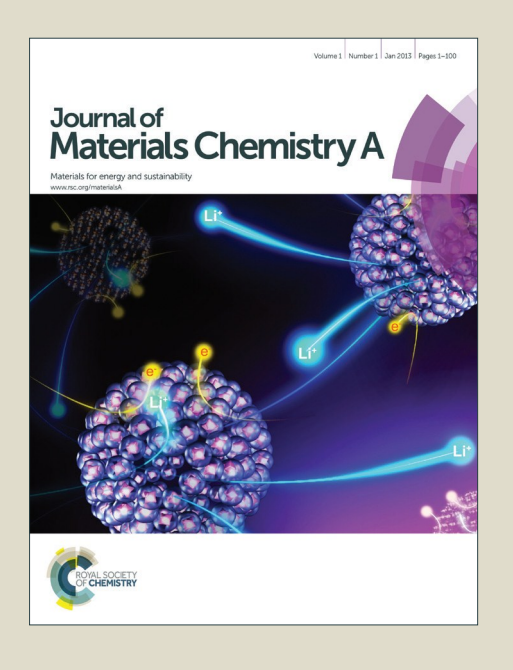
# Journal of Materials Chemistry A

Accepted Manuscript



This is an *Accepted Manuscript*, which has been through the Royal Society of Chemistry peer review process and has been accepted for publication.

Accepted Manuscripts are published online shortly after acceptance, before technical editing, formatting and proof reading. Using this free service, authors can make their results available to the community, in citable form, before we publish the edited article. We will replace this Accepted Manuscript with the edited and formatted Advance Article as soon as it is available.

You can find more information about *Accepted Manuscripts* in the **Information for Authors**.

Please note that technical editing may introduce minor changes to the text and/or graphics, which may alter content. The journal's standard <u>Terms & Conditions</u> and the <u>Ethical guidelines</u> still apply. In no event shall the Royal Society of Chemistry be held responsible for any errors or omissions in this *Accepted Manuscript* or any consequences arising from the use of any information it contains.





# **ARTICLE**

# Three-dimensional crumpled graphene as an electro-catalyst support for formic acid electro-oxidation

Received 00th January 20xx, Accepted 00th January 20xx

DOI: 10.1039/x0xx00000x

www.rsc.org/

Yang Zhou,\* Xian-Chao Hu, Qizhe Fan, and He-Rui Wen\*

Three-dimensional crumpled graphene (PRGO) was synthesized from graphene oxide (GO) solution with spay drying method and employed as the support material for Pd catalyst. The as-prepared catalysts were characterized by X-ray diffraction (XRD), scanning electron microscopy (SEM), tunnel electron microscopy (TEM) and X-ray photoelectron spectroscopy (XPS). The electro-catalytic activity and stability toward formic acid oxidation was investigated with cyclic voltammetry (CV) and chronoamperometry (CA), which indicated that Pd/PRGO catalyst exhibits larger electrochemically active surface area and mass activity as well as higher long term-stability in comparison to the commercial Pd/C and Pd/RGO catalysts. The enhanced catalytic performance is attributed to the high specific surface area of the 3D formation and utilization efficiency of Pd during the oxidation of formic acid.

# 1. Introduction

Recently, formic acid has attracted great attentions as a promising alternative fuel for liquid fuel cells because of its many advantages, such as reduced toxicity, higher kinetic activity and lower fuel crossover through Nafion membranes than methanol. It has been proved that the Pd catalyst exhibits excellent activity and stability towards the formic acid electro-oxidation (FAEO) compared with those of the Pt catalyst, which has relatively lower cost and higher resistance to CO poisoning. However, further investigations have demonstrated that the Pd catalyst has its drawbacks such as poor stability due to dissolution during the FAEO. Consequently, the activity and stability of the Pd-based catalysts still need further improvements to meet the demand of the direct formic acid fuel cell (DFAFC).

One of the best strategies to obtain alternative economical catalysts with desired performance is to effectively control the size and morphology of Pd nanostructure with a large specific surface area. Previous studies have proven that various Pd catalysts including Pd nanowire networks, Pd nanorods with high-index facets, concave Pd nanocubes and tetra-hexahedral Pd nanocrystals have extremely high activity towards the oxidation of ethanol and formic acid. Nevertheless, it is well known that the catalytic activity of metal catalyst is also related to the support materials besides the size and shapes of metal nanostructure. Various carbon materials such as carbon nanotube (CNT), carbon black, carbon nanofibers

<sup>11</sup> and graphene have been extensively investigated for the

Spray drying is widely used to prepare powders because of its many advantages, such as high efficiency, low preparation temperature and the fact that it can be scaled up to ton quantities. Herein, we report an efficient synthesis of 3D structured graphene with a porous structure from graphene oxide (GO) by spray drying. The fabricated 3D structured graphene decorated with Pd catalyst displays higher electro-catalytic activity and durability than 2D structured graphene decorated with Pd catalyst in DFAFC.

#### 2. Experimental

# 2.1 Synthesis of electro-catalysts

Graphene oxide was prepared by the oxidation reaction of graphite powder (99.9 % purity, Alfa Aesar, USA) using a modified Hummers' method.  $^{16,17}$  In a typical synthesis, 1 g of graphite powder was put into 23 mL of concentrated  $\rm H_2SO_4$  under magnetic stirring in an ice bath. The temperature of the

support materials in fuel cells due to its high specific surface area and conductivity. Especially, graphene (GR) has gained much attention as the support materials in DFAFC because of its high electron conductivity, large surface area, sufficient porosity and thermal stability. For example, Zhong et al. reported that the Pd nano-leaves supported on the reduced graphene oxide (RGO) exhibited excellent electro-catalytic performance towards the formic acid oxidation. But two-dimensional (2D) layered graphene have a tendency to form aggregation during the drying stage due to the  $\pi-\pi$  stacking and van der Waals attraction. The stacking of 2D GR-based sheets leads to reduce the specific surface area and utilization efficiency of Pd. Therefore, many efforts are needed to prevent severe stacking in 2D GR-based sheets.

<sup>&</sup>lt;sup>a.</sup> School of Metallurgy and Chemical Engineering Jiangxi University of Science and Technology 86 Hongqi Road, Ganzhou 341000, PR China E-mail: yangzhou1998@126.com

b. Research Center of Analysis and Measurement Zhejiang University of Technology 18 Chaowang Road, Hangzhou 310032, PR China

mixture was kept below 20 °C. The mixture was then stirred at 35 °C for 2 h. 46 mL of deionized water was added and the temperature was maintained at 96 °C for 15 min. After 46 mL of deionized water and 46 mL of 30 wt %  $\rm H_2O_2$  solution were added to the solution, the mixture was filtered and washed with 1 M HCl and distilled water until the rinse water became neutral. The product was finally freeze-dried, which was denoted as GO.

For the fabrication of 3D structured graphene, 1000 mL aqueous suspensions of GO at concentrations of 0.25 mg mL<sup>-1</sup> were prepared. After being ultrasonicated for 30 min, the combined solution were handled by spray drying using SD1000 spray dryer (EYELA) under the blower flux of 0.7 m $^3$ ·min $^{-1}$ , feeding speed of 300 mL·h $^{-1}$  and inlet temperature of 200  $^{\circ}$ C. The as-prepared product was designated as PRGO.

Subsequently, Pd/PRGO catalyst was prepared through the improved liquid phase reduction method. In a typical procedure, 50 mg of the as-prepared PGO support and 23.5 mL of 5 mM PdCl $_2$  solution was dispersed in 50 mL of water by sonication. After the pH was adjusted to nearly 9 using 1 M Na $_2$ CO $_3$  solution, a freshly prepared 10 mL of 0.1 M NaBH $_4$  solution was added to the solution, followed by stirring for 2 h. The resulting solution was filtered, washed, and dried at 85 °C for 10 h in a vacuum oven, yielding 20 wt % Pd loading on the supports. For comparison, Pd supported on GO catalyst with the same Pd loading amounts was prepared by the same procedure above, which was denoted as Pd/RGO. A commercial 10 wt % Pd/C (JM Pd/C) was purchased from Johnson Matthy Co., Ltd. and used as contrast samples.

#### 2.2 Characterizations

The phases present in the synthesized materials were identified using XRD (Panalytical X'Pert Pro, Cu K $\alpha$ 1 radiation source ( $\lambda$  = 0.1541 nm), voltage of 40 kV, current of 40 mA). The morphology and structure of the products were characterized using FE-SEM (Hitachi S-4700 II) and TEM (Tecnai G2 F30) with Energy-dispersive X-ray spectroscopic (EDS). XPS was carried out on Kratos AXIS Ultra DLD. All XPS spectra were corrected using the C 1s line at 284.6 eV. Curve fitting and background subtraction were accomplished.

#### 2.3 Electrochemical measurements

The electrochemical measurements were performed using a three-electrode cell with an Ivium electrochemical workstation at room temperature. For electrode preparation, 2 mg of electrocatalysts were ultrasonically mixed in 200 µl of ethanolwater solution to form a homogeneous ink followed by dropping 2 µl of the electrocatalyst ink onto the surface of a glassy carbon electrode (GCE, with a diameter of 3 mm), and 5 μl of Nafion solution of 1.0% (DuPont, USA) in ethanol was added to fix the electrocatalyst on the GCE surface. Glassy carbon (GC) disk electrode served as the substrate for the support. Prior to use, the GC electrode was polished using aqueous alumina suspension. And then the catalyst suspension was pipetted using a micropipettor onto the GC surface to make a Pd loading of about 0.056 mg cm<sup>-2</sup>. A Pt foil and saturated calomel electrode (SCE) were used as counter and reference electrodes, respectively. The electrocatalytic activity

of the catalysts on the oxidation of methanol was studied in 0.5 M  $\rm H_2SO_4$  aqueous solution containing 1.0 M HCOOH at a scan rate of 50 mV s<sup>-1</sup>.

#### 3. Results and Discussion

#### 3.1 Structure and Morphology

The XRD patterns of the as-prepared samples are shown in Fig. 1a and b. The diffraction peak at 11° is characteristic of the GO plane, suggesting the transformation to 2D layered graphene. 18 After spay-drying treatment, the graphene characteristic peak of the (002) plane is obviously found to decrease in the PRGO support. In addition, the  $2\theta$  values of the (002) peak for the PRGO is obviously shifted to lower diffraction angles in comparison with the GO. This behavior is related with the aggregation and restacking of graphene sheets being effectively prevented by spay-drying treatment. 19 The diffraction peaks at 40.6°, 46.2°, 67.8° and 81.4° are corresponded to the (111), (200), (220) and (311) lattice planes of the fcc crystalline Pd [JCPDS no. 46-1043], respectively.<sup>20</sup> According to Debye-Scherrer's formula, the crystal sizes of Pd nanoparticles are respectively calculated to be 6.3 and 4.8 nm for Pd/RGO and Pd/PRGO catalysts.21

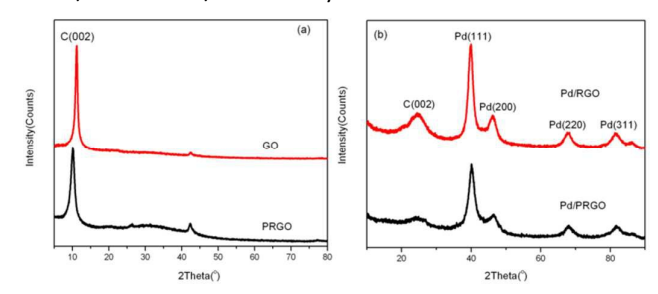


Fig.1 (a) XRD patterns of GO and PRGO; (b) XRD patterns of Pd/PRGO and Pd/RGO

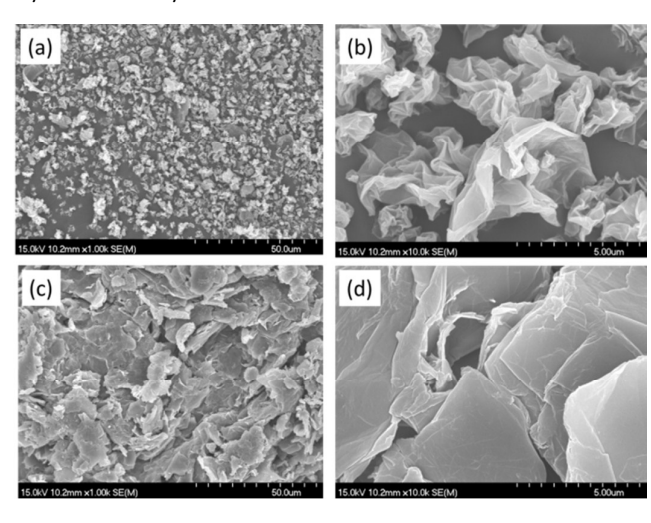


Fig.2 SEM images of (a-b) PRGO and (c-d) GO

The structure and morphology of the different samples were analyzed by the scanning electron microscopy (SEM) and

tunnel electron microscopy (TEM). Fig. 2 displays SEM images of GO and PRGO with different magnifications. SEM images (Fig. 2a and b) illustrates that the as-prepared PRGO has a 3D morphology, which appear as crumpled paper balls with diameters of about 3-5  $\mu m$ . Fig 2c and d are the SEM images of GO, it can be seen that 2D layered graphene sheets tend to form aggregation and stacking. Fig.3 presents TEM images and particle size distributions of Pd/PRGO and Pd/RGO catalysts. It can be seen from the TEM images that Pd particles on the PRGO support are smaller and more uniformly dispersed than those on the GO supports. The average sizes of particles in the Pd/PRGO and Pd/RGO catalysts are estimated from their histograms as being approximately 4.6 and 6.8nm, respectively, which are consistent with the results of XRD. In order to further investigate the structure and morphology of Pd nanoparticles on the surface of PRGO, the high-resolution TEM (HR-TEM) were carried out. Fig. 4a exhibits a lattice spacing of 0.23 nm with the lattice orientation of (111) of Pd, which indicates that Pd nanoparticles with an average size of 3-5 nm are dispersed on the surface of PRGO consistent with the XRD result. Energy-dispersive X-ray (EDX) analysis was also performed to study the chemical composition of Pd/PRGO catalyst. The existence of O element is considered to the oxygenated groups of PRGO. The EDS spectra of Pd/PRGO (Fig. 4b) confirms that the Pd loading concentration of 19.65 %, which is close to actual loading amounts of Pd

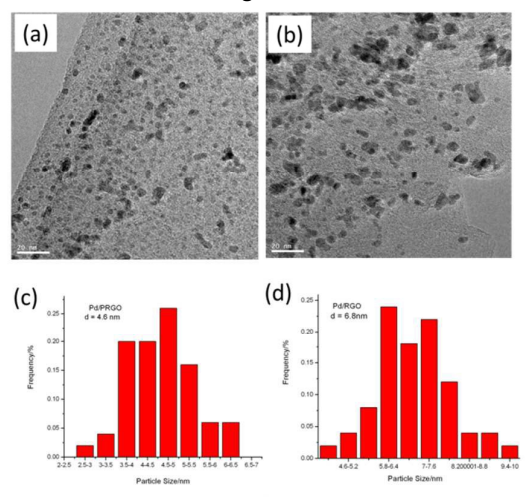


Fig. 3 TEM images of (a) Pd/PRGO, (b) Pd/RGO, (c) and (d) Pd particle size distributions of Pd/PRGO and Pd/RGO

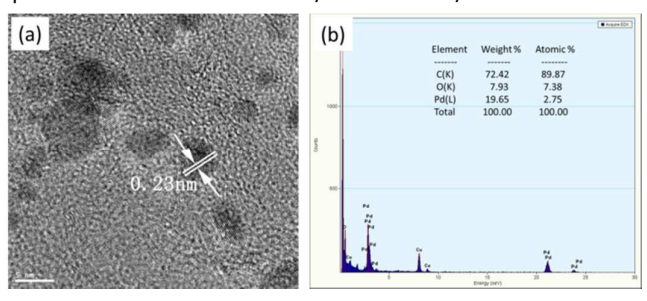


Fig. 4 high resolution (a) TEM image and (b) EDX spectrum of Pd/PRGO catalyst

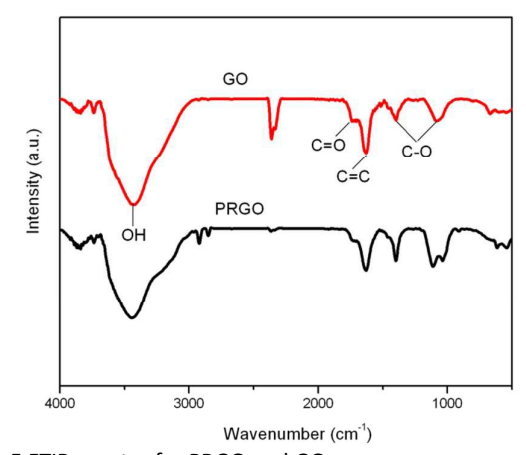


Fig. 5 FTIR spectra for PRGO and GO

According to the FTIR spectra of GO and PRGO (Fig. 5), the characteristic peaks at 3450 cm<sup>-1</sup>, 1620 cm<sup>-1</sup>, 1400 cm<sup>-1</sup> and 1083 cm<sup>-1</sup> are corresponded to –OH, C=C and C=O functional groups, respectively, indicating that the existence of carboxyl and hydroxyl groups on the graphene oxide surface. After spaying-dry treatment, all the characteristic peaks remain unchanged, which indicate that spaying-dry has not an effect on the surface composition of GO. X-ray photoelectron spectroscopy (XPS) was carried out in order to further evaluate the chemical composition of Pd/RGO and Pd/PRGO catalysts. Fig. 6 shows the XPS spectra of C 1s and Pd 3d photoemission from Pd/RGO and Pd/PRGO catalysts, respectively. As shown in Fig. 6, the main peak fitting at 284.7 eV is attributed to the C-C bond, the other small peaks are attributed to the - COOH (288.9 eV), -C-O-C- (286.8 eV) and - C-OH (285.6 eV) functional groups, which is consistent with the result of IR spectra.<sup>22</sup> In addition, two main characteristic peaks with binding energies of 335.6 and 340.9 eV are characteristic of the metallic Pd , and the other two peaks at 337.2 and 342.9 eV can be assigned to Pd<sup>2+</sup> in PdO and Pd(OH)<sub>2</sub>-like species,<sup>23</sup> suggesting the presence of Pd mainly exists in the form of the metallic state

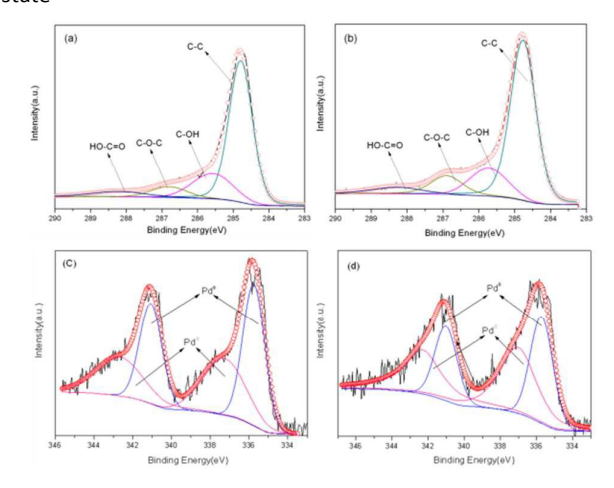


Fig. 6 XPS spectra of C1s for (a) Pd/RGO and (b) Pd/PRGO catalysts, Pd 3d for (c) Pd/RGO and (d) Pd/PRGO

#### 3.2 Activity toward formic acid oxidation

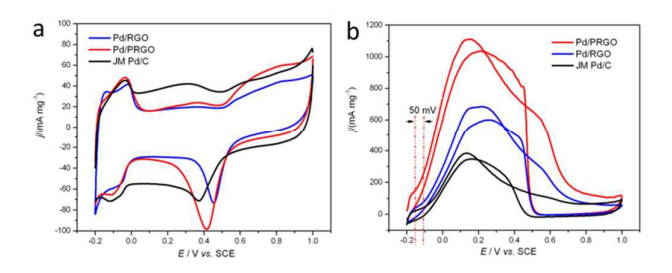


Fig. 7 a) Cyclic voltammetric curves of Pd/PRGO, Pd/RGO and JM Pd/C in 0.5 M  $\rm H_2SO_4$  at the scan rate of 20 mV s<sup>-1</sup>; b) Cyclic voltammetric curves of Pd/PRGO, Pd/RGO and JM Pd/C in 0.5 M  $\rm H_2SO_4 + 1$  M HCOOH solution at the scan rate of 50 mV s<sup>-1</sup>

The electro-catalytic activity of Pd/PRGO catalyst towards formic acid was investigated and further compared with JM Pd/C and Pd/RGO catalysts. First, the electrochemical active surface area (ECSA) of three catalysts were estimated by the cyclic voltammogram (CV) recorded in a N<sub>2</sub>-saturated solution of 0.5 M H<sub>2</sub>SO<sub>4</sub> at a scanning rate of 20 mV s<sup>-1</sup> (Fig. 7a). The ECSA can be calculated by the integrated area in the range -0.2 to 0.1 V attributed to the hydrogen adsorption/desorption regions after double-layer correction and assuming a value of 210  $\mu C$  cm<sup>-2</sup> for the adsorption of a hydrogen monolayer.<sup>24-27</sup> The calculated values of Pd/PRGO (40.9 m<sup>2</sup> g<sup>-1</sup>) are the highest in comparison with those of Pd/RGO (28.3 m<sup>2</sup> g<sup>-1</sup>) and JM Pd/C (20.0 m<sup>2</sup> g<sup>-1</sup>), which is due to the introduction of 3D structured graphene, thereby enhancing the dispersion of Pd nanoparticles on the surface of PRGO. <sup>22</sup>

The catalytic performance of three catalysts towards formic acid oxidation was investigated in 0.5 M H<sub>2</sub>SO<sub>4</sub> containing 1 M HCOOH. It is well known that the prominent peak range from 0.1 to 0.2 V is ascribed to the dehydrogenation reaction (direct pathway, HCOOH ----> CO<sub>2</sub> + 2H<sup>+</sup> + 2e), while the weak peak at approximately 0.6 V is related to the dehydration reaction (indirect way, HCOOH  $CO_{ads} + H_2O \longrightarrow CO_2 + 2H^+ + 2e$ ). Consequently, it can be concluded from Fig. 7b that the formic acid oxidation on these Pd-based electrocatalysts is mainly through the direct electron transfer pathway.<sup>30</sup> It can also be seen from Fig. 7b that the mass specific current of Pd/PRGO catalyst is 1112 mA·mg<sup>-1</sup> Pd, which is about 1.6 times that of Pd/RGO (683 mA·mg<sup>-1</sup> Pd) and 2.8 times that of JM Pd/C catalyst (386 mA·mg<sup>-1</sup> Pd). In addition, the onset potential of formic acid oxidation on the Pd/PRGO shifts negatively 50 mV compared to JM Pd/C and Pd/RGO. The higher formic acid oxidation current and lower onset potential indicate that Pd/PRGO catalyst has much better electrocatalytic activity due to its larger ECSA and the presence of PRGO enhances the utilization efficiency of Pd during the oxidation of formic acid.

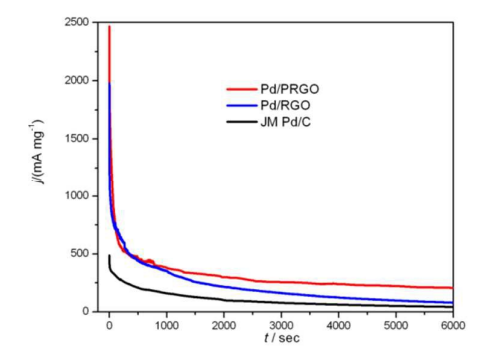


Fig. 8 Chronoamperometric curves of Pd/PRGO, Pd/RGO and JM Pd/C at 0.1 V in 0.5 M  $\rm H_2SO_4 + 1~M~HCOOH~solution$ 

The long-term stability and durability of three catalysts were further investigated by chronoamperometry tests (Fig. 8). All catalysts display an initial obvious current decay before reaching a quasi-equilibrium steady state because of dissolution and the formation of the poisonous species CO<sub>abs</sub>. The current decay rates of Pd/PRGO and Pd/RGO are much slower than JM Pd/C due to the presence of residual oxygen functional groups on graphene sheets can promote the oxidation of CO<sub>ads</sub> on the active Pd sites. <sup>31,32</sup> In addition, the Pd/PRGO catalyst exhibits higher current density and long-term performance compared with the Pd/RGO catalyst. This result confirms that the 2D catalyst has a low abilities and catalytic properties due to the stacked layers of the GR sheets.

#### 4. Conclusions

In summary, we have presented a spay-drying approach to synthesize a three-dimensional crumpled graphene material. Owing to the unique textual features, a 3D structured graphene supported Pd catalyst shows a greater catalytic surface area, greater electro-catalytic activity and greater steady-state current than Pd/RGO and JM Pd/C catalysts toward formic acid electro-oxidation. The improved catalytic activity of the Pd/PRGO catalyst is most likely due to the high specific surface area of the 3D formation together with and utilization efficiency of Pd during the oxidation of formic acid. We believe that the 3D structured graphene has promising applications as a catalyst support in fuel cells and its applications can be extended to other fields such as catalysis, sensors and energy storage.

#### **Acknowledgements**

The research was financially supported by the Jiangxi Ganpo 555 Project for Excellent Talents, National Natural Science Foundation of China (No. 51404110 and 21506187), Jiangxi Natural Science Foundation of China (No. 20151BAB213011), researching fund of Jiangxi University of Science and Technolo gy ( NSFJ2015-G08)

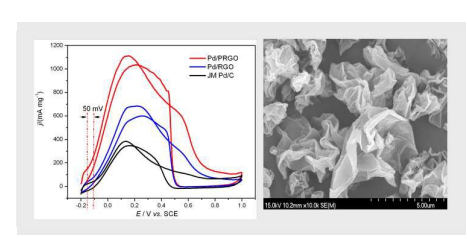
#### **Notes and references**

- D. Bin, B. B. Yang, F. F. Ren, K. Zhang, P. Yang and Y. K. Du, J Mater Chem A, 2015, 3, 14001-14006.
- H. D. Jang, S. K. Kim, H. Chang, J. H. Choi, B. G. Cho, E. H. Jo, J. W. Choi and J. X. Huang, *Carbon*, 2015, 93, 869-877.
- Y. Z. Lu and W. Chen, Journal of Physical Chemistry C, 2010, 114, 21190-21200.
- V. Mazumder, M. F. Chi, M. N. Mankin, Y. Liu, O. Metin, D. H. Sun, K. L. More and S. H. Sun, *Nano Lett*, 2012, 12, 1102-1106.
- 5. J. J. Wang, Y. G. Chen, H. Liu, R. Y. Li and X. L. Sun, Electrochemistry Communications, 2010, 12, 219-222.
- N. Tian, Z. Y. Zhou and S. G. Sun, Chemical Communications, 2009, DOI: 10.1039/b819751b, 1502-1504.
- J. W. Zhang, L. Zhang, S. F. Xie, Q. Kuang, X. G. Han, Z. X. Xie and L. S. Zheng, Chemistry-a European Journal, 2011, 17, 9915-9919.
- 8. N. Tian, Z. Y. Zhou, N. F. Yu, L. Y. Wang and S. G. Sun, Journal of the American Chemical Society, 2010, 132, 7580-+.
- Z. Z. Zhu, Z. Wang and H. L. Li, Applied Surface Science, 2008, 254, 2934-2940.
- 10. H. Y. Qian, H. J. Huang and X. Wang, *Journal of Power Sources*, 2015, **275**, 734-741.
- 11. D. Liu, Q. H. Guo, H. Q. Hou, O. Niwa and T. Y. You, *Acs Catalysis*, 2014, **4**, 1825-1829.
- 12.M. J. Allen, V. C. Tung and R. B. Kaner, *Chem Rev*, 2010, **110**, 132-145
- 13. o. Zhong, D. Bin, F. Ren, C. Wang, C. Zhai, P. Yang and Y. Du, *Colloids and Surfaces A: Physicochemical and Engineering Aspects*, 2016, **488**, 6.
- 14. J. Y. Luo, H. D. Jang, T. Sun, L. Xiao, Z. He, A. P. Katsoulidis, M. G. Kanatzidis, J. M. Gibson and J. X. Huang, *Acs Nano*, 2011, 5, 8943-8949.
- 15. Y. Zhou;, X. Hu;, Y. Xiao; and Q. Shu, *Electrochimica Acta*, 2013, **111**, 588-592.
- 16. H. WS; and O. RE, J Am Chem Soc, 1958, 80, 1339.
- 17. L. J. Cote, F. Kim and J. X. Huang, *Journal of the American Chemical Society*, 2009, **131**, 1043-1049.
- Y. C. Li, L. Zhang, Z. F. Hub and J. C. Yu, *Nanoscale*, 2015, 7, 10896-10902.
- J. Zhao, Z. S. Liu, H. Q. Li, W. B. Hu, C. Z. Zhao, P. Zhao and D. L. Shi, *Langmuir*, 2015, 31, 2576-2583.
- 20. R. R. Yue, H. W. Wang, D. Bin, J. K. Xu, Y. K. Du, W. S. Lu and J. Guo, *J Mater Chem A*, 2015, **3**, 1077-1088.
- 21. X. C. Hu, Y. Zhou, H. R. Wen and H. M. Zhong, *Journal of the Electrochemical Society*, 2014, **161**, F583-F587.
- 22. A. Halder, S. Sharma, M. S. Hegde and N. Ravishankar, *Journal of Physical Chemistry C*, 2009, **113**, 1466-1473.
- Y. Li, X. B. Fan, J. J. Qi, J. Y. Ji, S. L. Wang, G. L. Zhang and F. B. Zhang, *Nano Res*, 2010, 3, 429-437.
- 24. A. Pozio, M. De Francesco, A. Cemmi, F. Cardellini and L. Giorgi, *Journal of Power Sources*, 2002, **105**, 13-19.
- F. H. B. Lima and E. A. Ticianelli, *Electrochimica Acta*, 2004, 49, 4091-4099.

- 26. H. Zhao, J. Yang, L. Wang, C. G. Tian, B. J. Jiang and H. G. Fu, *Chemical Communications*, 2011, **47**, 2014-2016.
- 27. C. X. Guo, L. Y. Zhang, J. W. Miao, J. T. Zhang and C. M. Li, *Adv Energy Mater*, 2013, **3**, 167-171.
- 28. R. S. Li, Z. Wei, T. Huang and A. S. Yu, *Electrochimica Acta*, 2011, **56**, 6860-6865.
- 29. M. S. El-Deab, A. M. Mohammad, G. A. El-Nagar and B. E. El-Anadouli, *Journal of Physical Chemistry C*, 2014, **118**, 22457-22464
- 30. R. F. Wang, S. J. Liao and S. Ji, *Journal of Power Sources*, 2008, **180**, 205-208.
- 31. J. Kua and W. A. Goddard, Journal of the American Chemical Society, 1999, 121, 10928-10941.
- S. Sharma, A. Ganguly, P. Papakonstantinou, X. P. Miao, M. X. Li, J. L. Hutchison, M. Delichatsios and S. Ukleja, *Journal of Physical Chemistry C*, 2010, 114, 19459-19466.

# **ARTICLE**

The three-dimensional crumpled (PRGO) graphene synthesized from graphene oxide (GO) solution with spay drying method and employed as the support material for Pd catalyst. The as-prepared Pd/PRGO catalyst exhibits the mass specific current is 1112 mA·mg<sup>-1</sup> Pd, which is about 1.6 times that of Pd/RGO (683 mA·mg<sup>-1</sup> Pd) and 2.8 times that of JM Pd/C catalyst (386 mA·mg<sup>-1</sup> Pd).



Yang Zhou,\*\*a Xian-Chao Hu, b
Qizhe Fan, a and He-Rui Wen\*\*a
Page No 01. – Page No 05.
Three-dimensional crumpled
graphene as an electro-catalyst
support for formic acid
electro-oxidation